Supplementary Information (SI) for Nanoscale Horizons.
This journal is © The Royal Society of Chemistry 2024

Supplementary Information

# Harnessing Silicon Carbide Nanowire Photoelectric Synaptic Device for Novel Visual Adaptation Spiking Neural network

Zhe Feng[1#], Shuai Yuan[2#], Jianxun Zou[1], Zuheng Wu[1*], Xing Li[1], Wenbin Guo[1], Su Tan[1], Haochen Wang[1], Yang Hao[1], Hao Ruan[1], Zhihao Lin[1], Zuyu Xu[1], Yunlai Zhu[1], Guodong Wei[2*], Yuehua Dai[1*]

[#]These authors contributed equally to this work.

[1] School of Integrated Circuits, Anhui University, Hefei, Anhui, 230601, China.
[2] Xi'an Key Laboratory of Compound Semiconductor Materials and Devices, School of Physics & Information Science, Shaanxi University of Science and Technology, Xi’an 710021, Shaanxi, China.

Corresponding Email: wuzuheng@ahu.edu.cn; wgd588@163.com; daiyuehua2013@163.com.

Supplementary Figure S1-S9

Supplementary Table 1

Supplementary Note 1

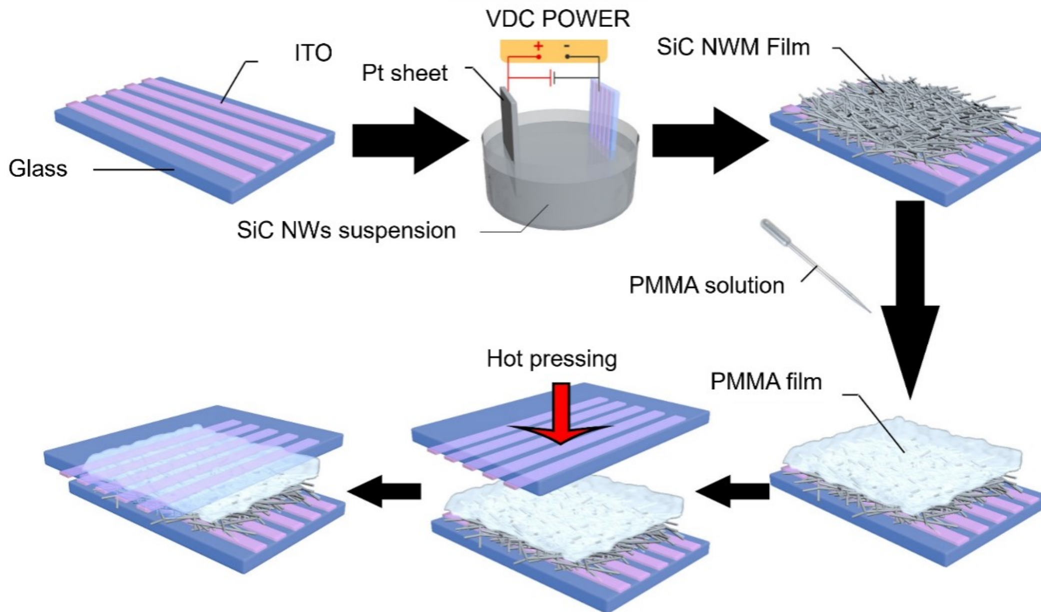


**Figure S1**. The prepared photoelectric synaptic device features a vertically stacked bilayer structure, consisting of a top ITO electrode, a PMMA layer, a SiC-NW thin film, and a bottom ITO electrode. The device fabrication process is as follows: First, 50 mg of SiC NWs, 75 *mg* of sodium dodecylbenzenesulfonate, 2.5 *mg* of aluminum nitrate, and 100 *mL* of isopropanol were mixed and subjected to ultrasonic treatment (ultrasonic power 800 *W*, 30 *min*) to obtain a SiC NWs deposition solution; subsequently, the SiC NW film was prepared on the ITO substrate using the EPD method, with deposition parameters set at 60 *V* for 6 *min*. After deposition, the ITO substrate with the SiC NW film was dried in a vacuum drying oven at 60 °*C* for 6 *h*. Then, 500 *μL* (0.1 *g/mL*) of PMMA solution was drop-cast onto the obtained SiC NW thin film, and the top ITO electrode was placed on top of the PMMA, at a 90-degree angle to the bottom ITO. Finally, the encapsulated device was obtained through a hot-pressing process (pressure ~6800 *Pa*, temperature 120 °*C,* 120 *s*).

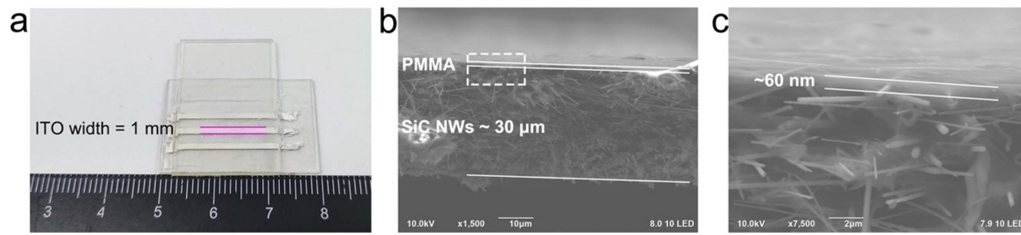


**Figure S2. a**. Optical photograph of the fabricated ITO/PMMA/SiC-NWs/ITO photoelectric synaptic devices. **b** and **c**. SEM profile of the PMMA/ SIC-NWS structure in a SiC NWs device.

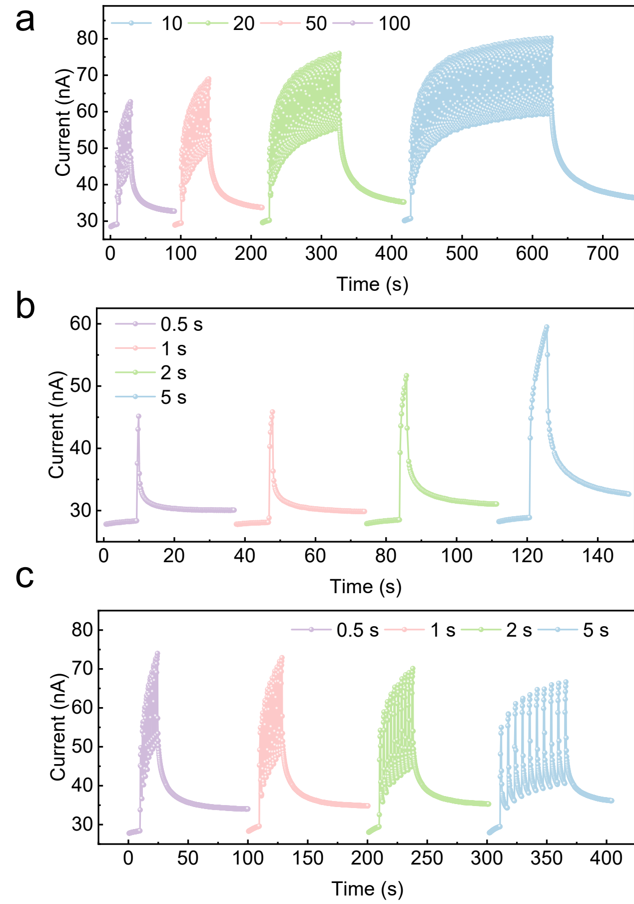


**Figure S3.** The controllable long-term plasticity of the photoelectric synaptic device under **a.** different light pulse number, and **b.** different light pulse width, and **c.** different light pulse frequency.

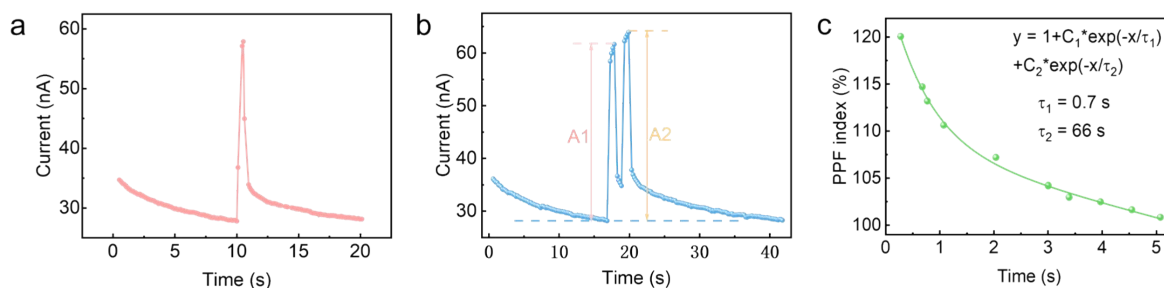


**Figure S4. a.** The *I-T* curve of the photoelectric synaptic device under 365 *nm* pulse light. **b.** The paired pulse facilitation (PPF) properties of the photoelectric synaptic device. **c.** PPF index versus time interval between two light pulses. The results indicate that the photoelectric synaptic device could also perform controllable short-term plasticity.

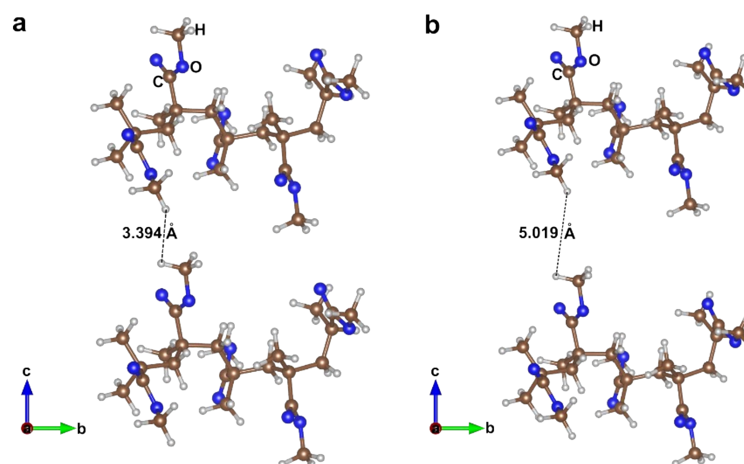


**Figure S5.** The PMMA molecular chains changes from initial of **a.** 3.394 *Å* to **b.** 5.019 *Å* after increase 30 *℃*.

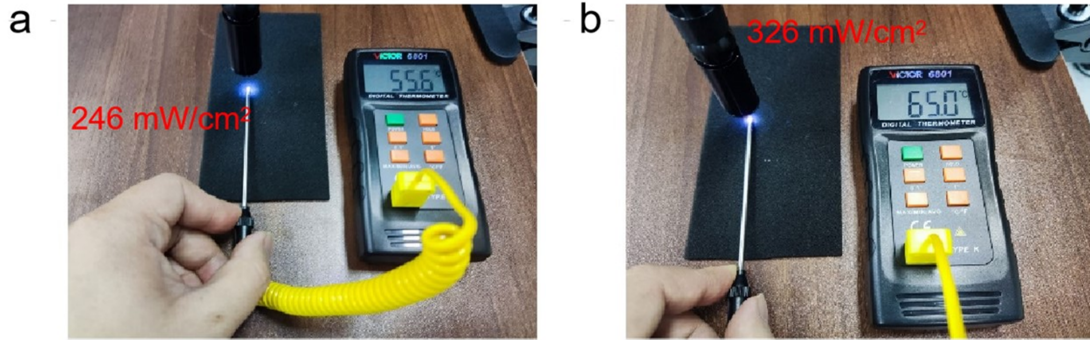


**Figure S6.** The temperature of 365 *nm* light at different power conditions **a.** 246 $mW/cm^2$ and **b** 326 $mW/cm^2$.

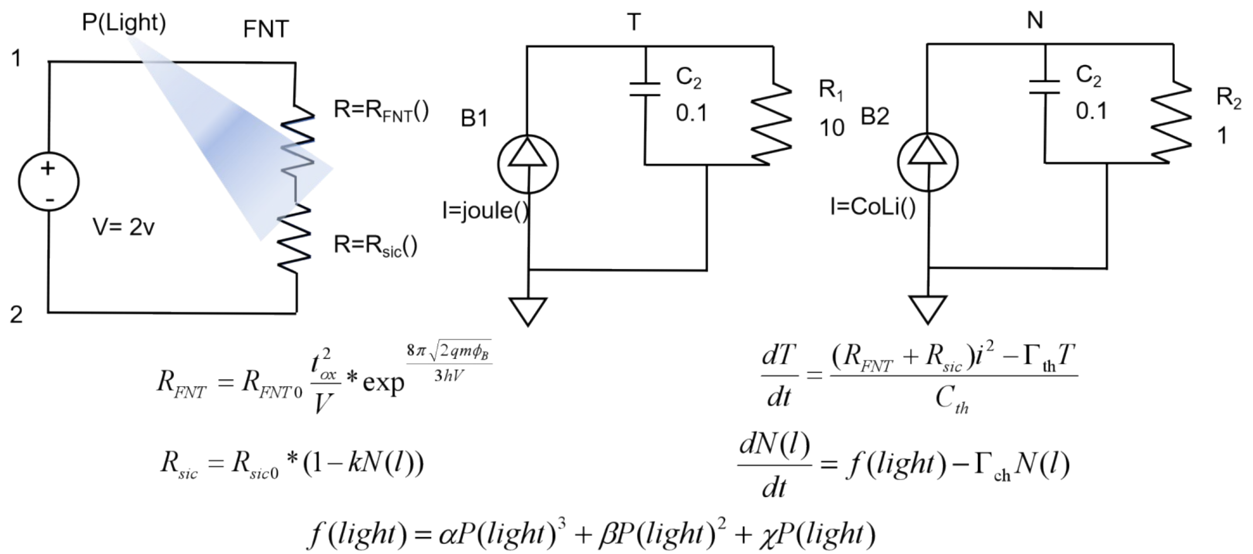


**Figure S7**. The photoelectric synaptic device's SPICE model.

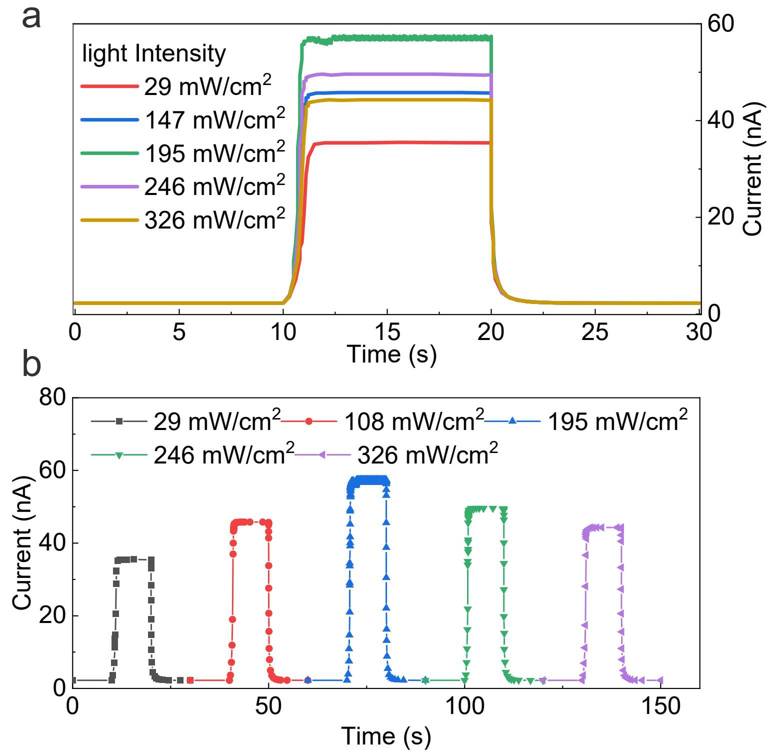


**Figure S8. a.** The response of the device model under light intensity stimulation. **b.** The spike pulse frequency of the circuit output under consecutive increasing light intensity stimulation.

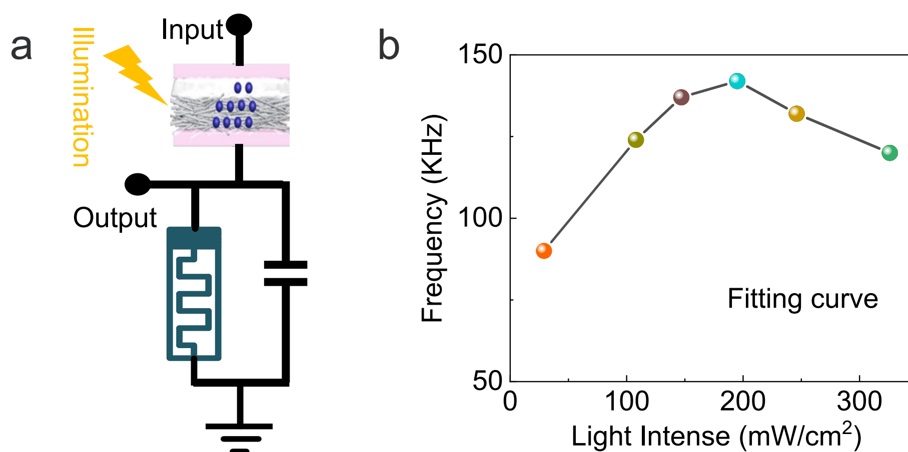


**Figure S9. a.** Schematic diagram of the VAAN circuit. **b.** The spiking frequency of the circuit output under increasing light intensity stimulation.

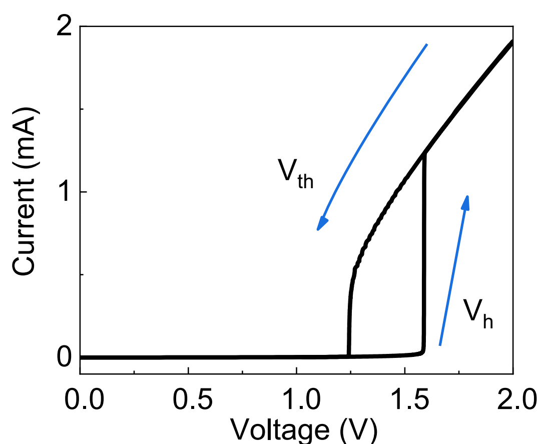


**Figure S10.** The *I-V* Response of threshold switching memristor model

**Table S1.** The influence of interchain spacing on HOMO and LUMO orbitals of PMMA molecular chains

| d (*Å*) | HOMO (*eV*) | LUMO((*eV*) | ΔE=LUMO-HOMO (*eV*) |
|---|---|---|---|
| 3.394 | -5.951 | -1.222 | 4.729 |
| 5.019 | -5.963 | -1.129 | 4.834 |

**Note 1. Modeling and Circuit-Level Simulation of Photoelectric Synaptic Devices**

The device is composed of PMMA resistors and SiC resistors, where the intermolecular distance of PMMA increases with temperature, and the concentration of photogenerated carriers is enhanced by illumination. Therefore, in this model, two state variables are designed: temperature and photogenerated carrier concentration. The concentration of photogenerated carriers is increased by illumination, and after the illumination is turned off, the photogenerated carrier dissipate, as shown in **Equation 1**.

$$\frac{dN(l)}{dt} = f(light) - \Gamma_{\mathrm{ch}} N(l) \#(1)$$

$$f(light) = \alpha P(light)^3 + \beta P(light)^2 + \chi P(light) \#(2)$$

$N(l)$ represents the concentration of photogenerated carriers, and $f(light)$ is a function fitted to the intensity of illumination, as shown in **Equation 2**, where $\alpha$, $\beta$, and $\chi$ are the fitting coefficients, $P(light)$ is the optical power per unit area input, and $\Gamma_{\mathrm{ch}}$ is the photogenerated carrier recombination coefficient, indicating that the concentration of photogenerated carriers under illumination is jointly affected by the intensity of illumination and the recombination of photogenerated carriers.

$$R_{sic} = R_{sic0} * (1 - kN(l)) \#(3)$$

**Equation 3** states that the higher the concentration of photogenerated carriers, the lower the resistance of SiC, where $R_{sic}$ is the resistance at SiC, $R_{sic0}$ is the fitted resistance coefficient, and $k$ is the gain coefficient.

$$R_{FNT} = R_{FNT0} \frac{t_{ox}^2}{V} * \exp^{\frac{8\pi\sqrt{2qm\phi_B}}{3hV}} \#(4)$$

$$tox = dox + \xi T \#(5)$$

$$\frac{dT}{dt} = \frac{(R_{FNT} + R_{sic}) i^2 - \Gamma_{\mathrm{th}} T}{C_{th}} \#(6)$$

The resistance at PMMA is shown in **Equation 4**, where $R_{FNT}$ is the resistance at PMMA, $R_{FNT0}$ is the fitted resistance coefficient for PMMA, $V$ is the input voltage, $q$ is the charge, $m$ is the electron mass, $\varphi_b$ is the barrier, $h$ is Planck's constant, and $t_{ox}$ is the intermolecular distance at PMMA. **Equation 5** indicates that $t_{ox}$ changes with temperature, where $d_{ox}$ is the intermolecular distance of PMMA in the absence of light, and $\xi$ is a fitting coefficient. The **equation 6** describes the change in temperature; the temperature of the device is influenced not only by Joule heat but also by heat

dissipation, which is a combined effect of thermal conductivity $\Gamma_{th}$ and temperature. $C_{th}$ describes the overall thermal capacitance of the device.

A SPICE model is constructed based on these equations, as shown in **Figure S7**. Upon applying light stimulation (where light is applied to the device through hyperparameters), a device response is obtained by applying a 10*s* pulse width of light stimulation ranging from 29-326 $mW/cm^2$, as shown in **Figure S8a**. Additionally, by applying a series of 10*s* light pulses, the response obtained is shown in **Figure S8b**, demonstrating that the model can achieve a response that initially increases and then decreases with increasing light power, consistent with the device response. Furthermore, we incorporated the photoelectric synaptic device into traditional LIF neuron circuit to investigate the potential of developing VAAN with this device (**Figure S9a**). The results indicate that the VAAN could reliably exhibit visual adaption coding ability (**Figure S9b**). The results suggest that the VAAN is suitable for VASNN applications.

**Note 2. The threshold switching memristor model of artificial neuron circuit**

The threshold switching memristor model is based on the Poole-Frenkel conduction mechanism, consistent with previous research [S1], the formula is as follows.

$$R_m = R_0 e^{\frac{1}{kT_m}\left(E_a - q\sqrt{\frac{qE}{\pi\varepsilon_0\varepsilon_r}}\right)} \#(7)$$

$$\frac{dT_m}{dt} = \frac{R_m i_m^2 - \Gamma_{th}\Delta T}{C_{th}} \#(8)$$

**Equation 7** describes the device resistance $R_m$, which depends on the temperature $T_m$ as the state variable, where $R_0$ is fitting resistance coefficient, $k$ denotes Bolzmann's constant, $E_a$ represents the activation energy, $q$ is the electron charge, $\varepsilon_0$ is vacuum permittivity, $\varepsilon_r$ is relative permittivity, electric field $E = vm / tox$, $tox$ is oxide thickness, and $v_m$ is the voltage across memristor. The state **Equation 8** describes the evolution of temperature, accounting for the balance between the Joule heat generated by the device and its dissipation. Here, $C_{th}$ represents the thermal capacitance, $\Gamma_{th}$ denotes the thermal conductance.

When a DC sweep voltage is applied to the device, the threshold switching response can be observed, as shown in **Figure S10**. The device exhibits a threshold voltage ($V_{th}$) of approximately 1.6V and a holding voltage ($V_h$) of approximately 1.25V.

## References

S1. Radhakrishnan, J., et al. "A physics-based Spice model for the Nb2O5 threshold switching memristor." CNNA 2016; 15th International Workshop on Cellular Nanoscale Networks and Their Applications. VDE, 2016. https://www.vde-verlag.de/proceedings-en/564252025.html.